Scientific and clinical implications of heterogeneity in uveal melanoma

Lange, M.J. de

6

Preclinical analysis of Dasatinib in uveal melanoma xenografts

M.J. de Lange, F. Némati, M. el Filali, M. Versluis, R. de Wijn, A.G. Jochemsen, R. Ruijtenbeek, G.P.M. Luyten, M.J. Jager, D. Decaudin, P.A. van der Velden

Submitted

ABSTRACT

Purpose:

Uveal melanoma (UM) leads to metastasis in up to 50% of the patients. Patients at risk are readily identified using an array of prognostic markers but an effective treatment is lacking. GNAQ/GNA11 mutations are the common denominators of oncogene signaling in UM and Src is a likely downstream kinase. We describe the preclinical analysis of Dasatinib, a known inhibitor of Src kinase.

Experimental design

Seven short-term cultured tumors were exposed to Dasatinib and evaluated for proliferation and MAPK signaling. Additionally, Dasatinib treatment was investigated in vivo with four UM xenografts models. Xenografts were analyzed for MAPK signaling and Src kinase activity in order to identify potential biomarkers for treatment response.

Results

Dasatinib treatment of seven primary UM and two xenograft cell line cultures resulted in inhibition of phosphorylation of MAPK and Src kinase, but growth arrest was observed in only four of the seven cultured tumors. Of the four xenografts treated with Dasatinib the growth of two tumors was inhibited. MAPK and Src inhibition was observed in the xenografts upon Dasatinib treatment but this did not correlate with tumor growth inhibition. However, the non-responding UM xenograft could be recognized by a high kinase activity.

Conclusions

Dasatinib inhibits growth of a subset of UM in vitro and in vivo. Therefore this Src family kinase inhibitor, Dasatinib, is a treatment option for UM. Furthermore, kinase activity emerged as a potential biomarker for Dasatinib treatment.

INTRODUCTION

Uveal melanoma (UM) is a rare tumor affecting 7/1.0 million of the Western population per year [1]. Still, it is the most common tumor in the eye in adults; 30 % of the tumors is asymptomatic and only discovered at routine examination [2]. This malignancy ultimately leads to metastatic disease in up to 50% of the patients [3]. Most often metastases are found in the liver and once liver metastases have been detected, life expectancy is only 2-6 months since an effective treatment is lacking for these patients [4]. This highlights the necessity of effective adjuvant treatment for high risk patients and precision treatment options for metastasis patients.

Hotspot mutations in *GNAQ* and *GNA11* have been identified as primary event in UM development and is found in >80% of all UM [5,6]. These recurrent mutations make UM genetically homogeneous and attractive for precision medicine approaches. *GNAQ* and *GNA11* are proto-oncogenes that encode for the α-subunit of Gq class proteins. These proteins mediate the signal transduction of G protein coupled receptors and mutations eventually translate into mitogen-activated protein kinase (MAPK) activation. However, the pathways that are controlled by *GNAQ* and GNA11 in UM remain largely undefined. Protein kinase c (PKC) is a downstream member of *GNAQ/11* signaling and the PKC inhibitor Sotrastaurin reduces UM growth and increases survival [7,8]. Sotrastaurin is currently in clinical study for treatment of UM metastasis but other downstream factors are also possible treatment targets. Inhibitors of bcl-2, Rb, the phosphatidylinositol-3-kinase-AKT pathway and other tyrosine kinase inhibitors as treatment options for UM have been extensively described [9,10].

Mostly regarded as a final target in a kinase cascade, the MAPK pathway is important in many types of cancer and in UM this pathway was also found to be activated [11]. We identified Src as a possible upstream regulator of MAPK activation in UM, providing an opportunity for pharmaceutical intervention. Treatment of UM cell lines with experimental Src inhibitors reduced proliferation in vitro in a MAPK dependent manner [12].

Dasatinib is a broad range kinase inhibitor that inhibits Src-family kinases [13,14] and has been approved for the treatment of patients with BCR-ABL-positive chronic myeloid leukemia and Philadelphia Chromosome positive (Ph+) acute lymphoblastic leukemia [15]. Even though specificity is very low compared to other BCR-ABL inhibitors, Dasatinib treatment results in remission and improved survival in these malignancies [16]. For several other cancers including melanoma, Dasatinib is still under investigation [17].

We investigated in vitro and in vivo the efficacy of Dasatinib on UM tumor growth, phosphorylation status and kinase inhibition. We furthermore evaluated enzymatic kinase activity as a possible biomarker for Dasatinib treatment efficacy in UM xenograft models.

MATERIALS AND METHODS

Patient tumor material and primary cell cultures

Informed consent was obtained prior to enucleation and the study was performed according to the tenets of the Declaration of Helsinki. Diagnosis was based on the histopathology of the tumor samples. Hematoxylin-eosin-stained 4-µm sections were examined for cell type, largest basal diameter, prominence, ciliary body involvement and scleral invasion. Fresh tumor tissue, obtained immediately after enucleation of the eye, was used to isolate DNA, protein lysates and to develop a short-term cell culture (n=7). Histologic sections were prepared from tissues fixed in 4% neutral-buffered formalin for 48 hours and embedded in paraffin.

Primary tumor cell cultures and Dasatinib treatment

Primary UM cell cultures were cultured in Amniochrome® Pro Medium (Lonza Group Ltd, Basel, Switzerland) and incubated in an atmosphere with 5% CO2 at a temperature of 37oC. (HERAcell 240 CO2 Incubator, Thermo Fisher Scientific Inc, USA). The cells were passaged once or twice a week using 0.05% trypsin-EDTA.

Dasatinib (Toronto Research Chemicals Cat# D193600) (stock solution concentration of 20 mM in DMSO) was dissolved in Amniochrome® Pro Medium (Lonza Group Ltd.) to obtain concentrations of 200nM and 2µM and used in experiments as described. As control, we used standard Amniochrome® Pro Medium.

The effect of Dasatinib on UM cell viability was measured by mitochondrial activity using the water-soluble tetrazolium salt (WST-1) assay (Roche Diagnostics, Indianapolis, IN, USA). In short, UM cells were seeded into 96-well plates (1200 cells/well). After overnight adherence, cells were incubated with either regular medium or Dasatinib solutions (200nM to 2µM), and placed in an standard incubator (5% CO2, 37oC). After the indicated incubation time (1, 2, or 3 days) 10µl of WST-1 reagent was added to each well and after four hours of incubation, absorbance was measured at 450nm (n=7) on a multiwell spectrophotometer (Perkin Elmer, Wellesley, MA).

Xenograft models

Human uveal melanoma xenograft models were established from primary patient's surgical specimens by grafting tumor fragments into the interscapular fat pad of SCID mice and

maintained through in vivo passages. For experimental therapeutic assays, 4 patient derived xenografts (PDX) , MP34, MP41, MP46 and MP55, were grafted with a tumor fragment of 15 mm3. Mice bearing growing tumors with a volume of 48 to 288 mm3 were individually identified and randomly assigned to the control or treatment groups (7-10 animals per group), and treatment was started on day 1. Mice were treated with Dasatinib 50 mg/kg/day, 5 days/week, 4 weeks, p.o orally, or its excipients (control). Tumor volumes were calculated by measuring two perpendicular diameters with calipers. Each tumor volume (V) was calculated according to the following formula: V = a × b2 / 2, where a and b are the largest and smallest perpendicular tumor diameters. Relative tumor volumes (RTV) were calculated from the following formula: RTV = (Vx/V1), where Vx is the tumor volume on day x and V1 is the tumor volume at initiation of therapy (day 1). Growth curves were obtained by plotting the mean values of RTV on the Y axis against time (X axis, expressed as days after start of treatment). Antitumor activity was evaluated according to tumor growth inhibition (TGI), calculated according to the following formula: percent GI = 100 − (RTVt / RTVc × 100), where RTVt is the median RTV of treated mice and RTVc is the median RTV of controls, both at a given time point when the antitumor effect was optimal. Detail of antitumor efficacy and tumor characteristic can be found in Nemati et al. 2010 [18]. At the end of the study, 5 xenografts were collected from control mice and five from treated mice for each models. Additionally, two cell lines derived from xenografts were used to evaluate inhibition of phosphorylation of Src. These cell were kindly provided by and the description of these cells will be provided by manuscript in preparation Nabil Amirouchene et al.

PCR

GNAQ/GNA11 genes were amplified with a Polymerase Chain Reaction (PCR) using chromosomal DNA, isolated from frozen tumors using the QIAamp DNA minikit from Qiagen (Qiagen Inc, Turnberry Lane, Valencia, CA, United States). The following protocol was used for amplification of exon 5 of the *GNA11* and the *GNAQ* genes:

94°C, 1min; (96°C, 15sec; 63°C, 15sec; 72°C, 1min) 7X; (96°C, 15sec; 61°C, 15sec; 71°C, 1min) 8X; (96°C, 15sec; 60°C, 15sec; 72°C, 1min), 36X; 72°C, 1min, end.

The following primers were used for *GNA11* Forward: 5'-CGCTGTGTCCTTTCAGGATGGTG-3', and *GNA11* Reverse 5'-GCCCACCTCGTTGTCCGACT-3' and for *GNAQ* Forward: 5'-CCCTAAGTTTGTAAGTAGTGCTATATTTATGTTG-3', and *GNAQ* Reverse: 5'-ATGATAATCCATTGCCTGTCTAAAGAACAC-3'. After amplification, DNA clean-up was performed using the Nucleospin Extract II columns of Macherey-Nagel (Qiagen Inc.) following the manufacturers protocol. For sequencing analysis, samples were prepared by adding 10 pmol of reverse primer to the amplified DNA.

PamGene tyrosine-kinase peptide microarray

To ascertain tyrosine-kinase activity in lysates of xenografts, the PamChip-4 was used on a PamStation12 (PamGene B.V., 's Hertogenbosch, The Netherlands), as described previously [12]. In short, this array consists of 144 peptides spotted on a porous carrier. The 144 peptides are known tyrosine-kinase substrates and phosphorylation of these peptides by cell lysates is monitored by a fluorescein labeled PY20 which recognizes phosphorylated tyrosine. PamStation12 carries 3 chips providing 12 analyses simultaneously. We loaded 40 xenograft samples representing four different UM models, 20 control and 20 Dasatinib treated xenograft. The ATP concentration used was 100μM in all kinase activity measurements.

Western blot analysis

Cells were harvested in M-PER Mammalian Protein Extract Reagent (Pierce, Rockford, IL, USA), supplemented with 1% Halt Protease Inhibitor Cocktail, EDTA-free (Pierce) and 1% Halt Phosphatase Inhibitor Cocktail (Pierce). Protein concentrations were measured by using the BCA Protein Assay kit (Pierce).

Cell lysates, containing an equal amount of protein, were mixed with equal volumes of 6× sample loading buffer, boiled for 10 min, cooled on ice, and analyzed by 10% SDS polyacrylamide-gel electrophoresis (SDS-PAGE). Separated proteins were transferred to a PVDF low-fluorescence membrane (Millipore). Subsequently, the membrane was blocked with Li-Cor blocking buffer (Li-Cor biosciences, Lincoln, Nebraska, USA) for 1 h at room temperature and incubated with primary antibodies (rabbit anti-pSrc527, rabbit anti-pSrc416, rabbit anti-Src, rabbit anti-Erk1/2, mouse anti-pErk1/2, rabbit anti-GAPDH (loading control) (all from Cell Signaling, Boston, USA) followed by an infrared labeled secondary antibody (goat anti-rabbit800 and goat anti-mouse680 (both from Li-Cor)). Labeled PVDF membranes were scanned with the Li-Cor odyssey scanner and quantification of proteins was performed using the Li-Cor software.

Statistical analysis

Statistical analysis was performed using SPSS 20.0 software (SPSS Inc. Chicago, Illinois, USA). One-way ANOVA was used to analyze significant difference in cell proliferation of treated and untreated cells. Processing, visualization and analysis of kinase activity data obtained with the PamChip system was done using Bionavigator software (PamGene B.V.), interfaced to R (R foundation for statistical computing, Vienna, Austria) for advanced analysis methods such as principal component analysis (PCA). Fluorescent spots in the micro-array images were quantified and the local background corrected signals were obtained for each spot in each array. In order to remove peptides that only showed very low or absent signals, the time-course of the phosphorylation signal during the PamChip

incubation was examined. Signals were taken as positive if a significant positive trend ($p < 0.01$) could be detected during the incubation. Peptides that lacked such a signal in all samples were removed, leaving 109 peptides for further analysis, which was performed on signals obtained after a final washing step at the end of the incubation. Prior to further analysis signals were log2 transformed, hereto a small fraction of negative values was handled by setting values smaller than a suitably small number (here: 1) equal to that small number.

RESULTS

The application of the experimental Src inhibitors PP1 and PP2 has already shown that Src inhibition substantially reduces cell proliferation in UM cell lines [12]. The aim of this study was to analyze the efficacy of the clinically available Src kinase-inhibitor Dasatinib in models better reflecting primary UM.

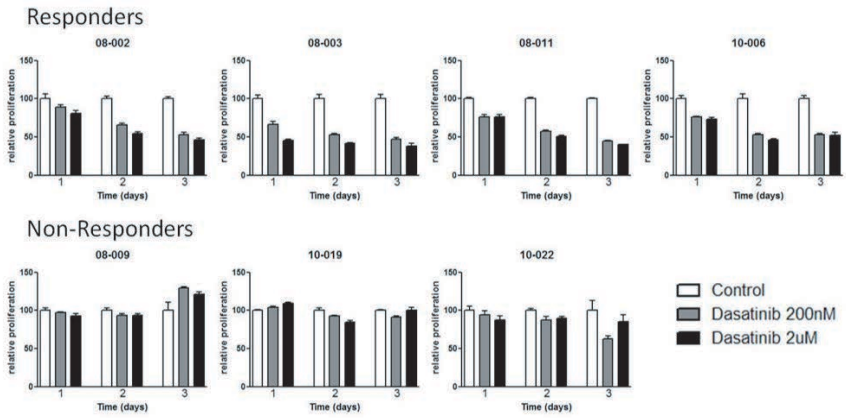

Figure 1. Cell viability of primary UM cell cultures treated with Dasatinib.
Cell viability was measured at three consecutive days. Each time point embodied a control culture and two Dasatinib treatments (200 nM and 2 μM). The untreated control culture is set at 100%.

Inhibition of UM growth by Dasatinib

Cell viability was significantly reduced by Dasatinib in a dose-dependent manner in four out of seven early passage UM cell cultures (Figure 1). Three cultures appeared Dasatinib resistant and displayed no growth inhibition upon treatment with either low (200nM) or high dose (2μM) of Dasatinib. Regardless of treatment response, in tested UM cultures a reduction of activated ERK (pERK) was observed (Figure 2a-b). Though, the degree of pERK down-regulation varied widely, no correlation can be made with responders and non-responders. Additionally, basal phosphor-ERK expression does not correlate with treatment response either.

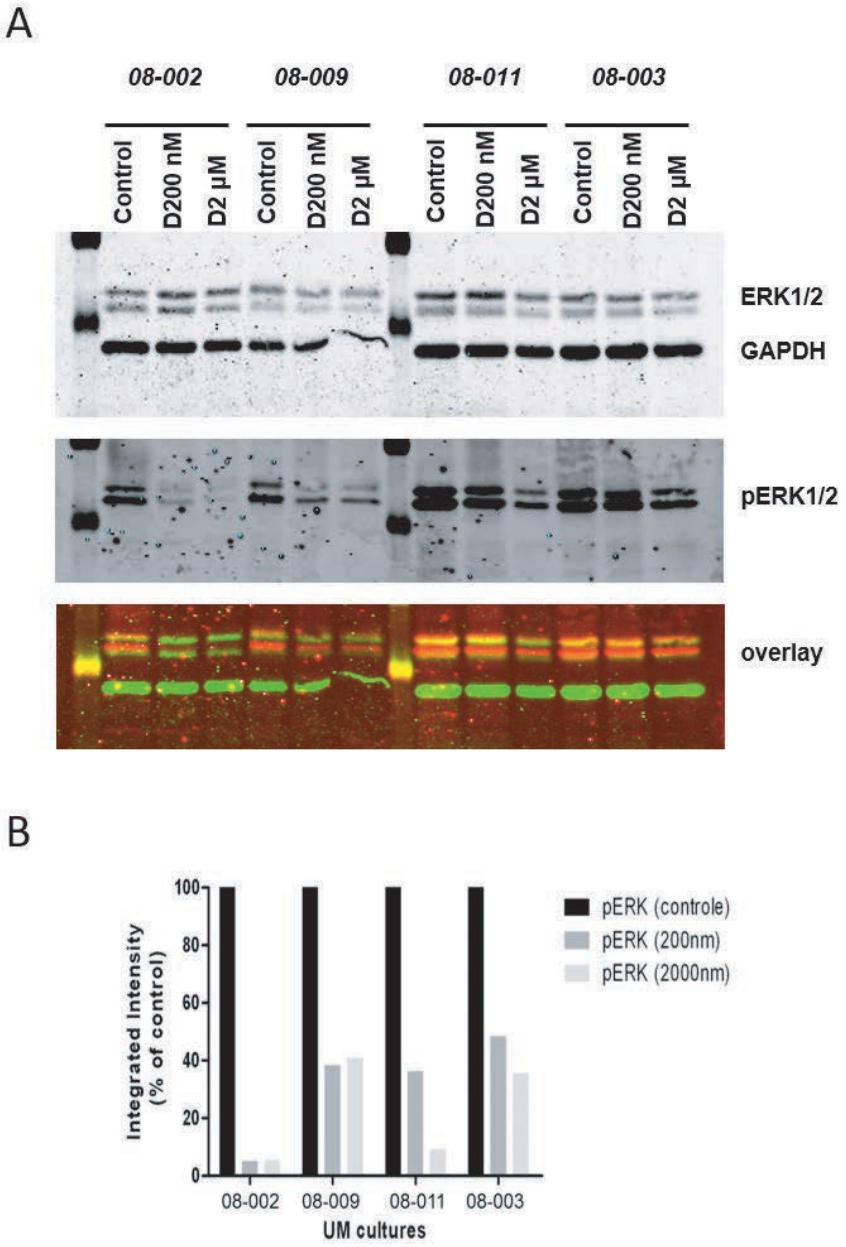

Figure 2. ERK/pERK analysis in UM cell cultures treated with Dasatinib.
ERK/phospho-ERK analysis of four representative UM cell cultures treated for 48 hours with Dasatinib, 200 nM and 2 µM. (a) Simultaneous incubation with total ERK (top) and pERK (middle) specific antibodies allows quantification of pERK relative to ERK (bottom). (b) Quantification of Western analysis by fluorescent staining intensity.

Molecular mechanisms

GNAQ and *GNA11* mutations represent early events in UM development that could be related to Src activity and Dasatinib efficacy in UM. However, mutations in *GNAQ/GNA11* are very common, and in only one tumor we could not detect a mutation mutation (10-006). Monosomy 3 is a late event and strongly correlated with metastasis development. All three growth non-responders displayed a normal chromosome 3 karyotype whereas two out of four responders displayed monosomy 3 (Table 1).

Table 1. Molecular characteristics and Dasatinib treatment sensitivity of seven primary UM cultures.

Primary tumor	*Mutation status*	*Chromosome 3*	*Response*
08-002	$GNAQ^{Q209L}$	N	R
08-003	$GNAQ^{Q209P}$	L	R
08-009	$GNA11^{Q209L}$	N	NR
08-011	$GNA11^{Q209L}$	N	R
10-006	-	L	R
10-019	$GNAQ^{Q209L}$	N	NR
10-022	$GNAQ^{Q209L}$	N	NR

Abbreviations: N = normal, L = loss. R = responder, NR = non-responder.

Table 2. Characteristics and Dasatinib treatment sensitivity of four xenograft models.

Models	Histopathology		Chromosome 3		Mutation status				Response	
					GNA11		**GNAQ**			
	P	**X**	**P**	**X**	**P**	**X**	**P**	**X**	**TG**	**KI**
MP34	E	E	-	L3p	+	+	0	0	R	R
MP41	E	E	N	N	+	+	0	0	R	R
MP46	E	M	L	Isodisomy	-	0	+	+	NR	R
MP55	M	E	L	L	+	+	0	0	NR	NR

Abbreviations: P = primary tumor; X = xenograft. E = epithelial, M = mixed. N = normal, L = loss. + = mutation, 0 = no mutation, - = not determined. TG = tumor growth, KI = kinase inhibition. R = responder, NR = non-responder.

Xenograft: inhibition of tumor growth

We used four UM xenografts models to assess treatment efficacy of Dasatinib in vivo (table 2). Control experiments were performed with four biological replicates for MP46, six replicates for MP41 and five replicates for both MP34 and MP55. Additionally, five biological replicates were used for all Dasatinib treated mice. Xenograft models MP34

and MP41 presented a decrease in tumor growth rate after treatment with Dasatinib. The growth of MP46 appeared slightly inhibited while MP55 did not show a response (Figure 3a).

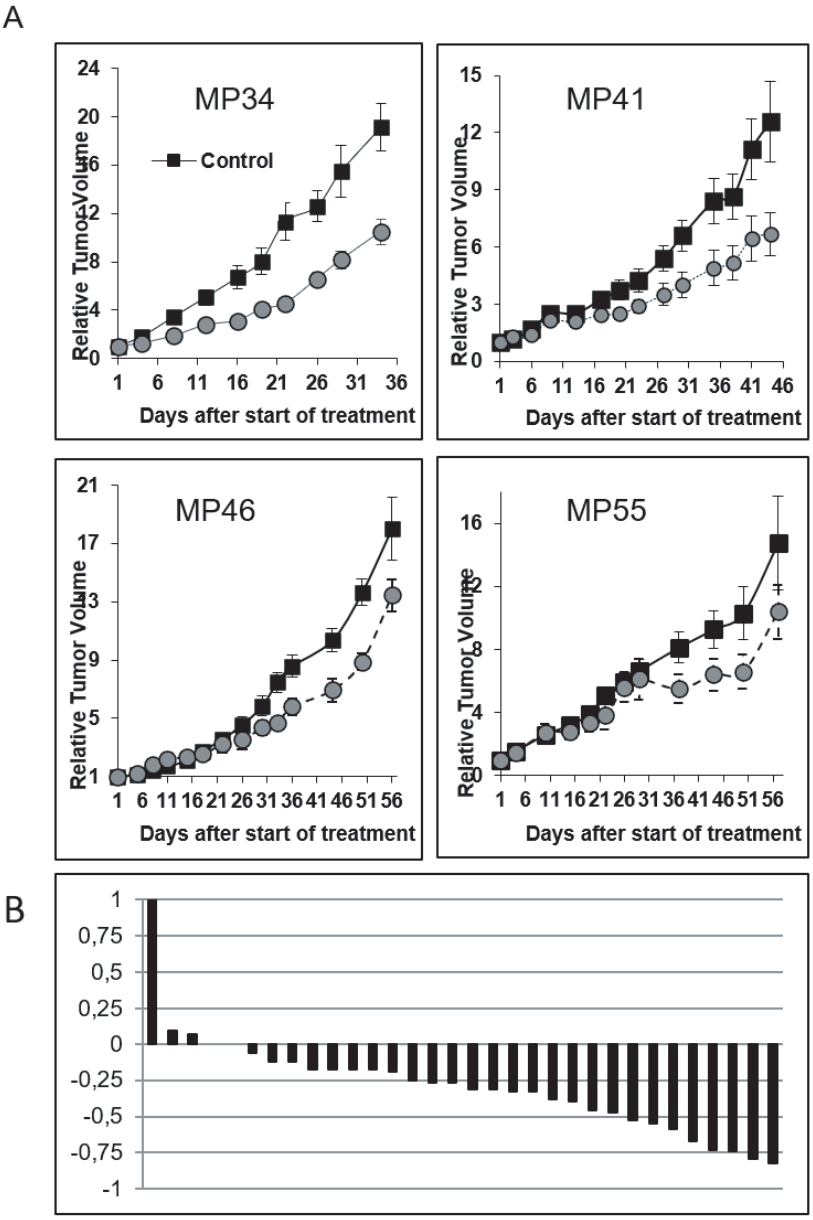

Figure 3. In vivo effect of Dasatinib on tumor volume of four xenografts models.
(a) Average tumor volume of four xenograft models treated with Dasatinib or mock-treated. Each point represents the average of 4-6 mice. (b) Individual mouse variability represented as relative tumor volume variation [(RTVV) -1] of each Dasatinib-treated mouse.

Additionally, to evaluate responses to Dasatinib observed in the 4 models according to individual mouse variability, we decided to consider each mouse as one tumor-bearing entity. In this, when relative tumor volume variation [(RTVV) -1] of each Dasatinib-treated mouse was calculated, regardless of the doses of Dasatinib, we observed that 84% of all Dasatinib-treated mice (27/32) had a negative ratio compared to control groups, and that 25% had a ratio lower than 50% (Figure 3b). To evaluate possible mechanisms underlying the different treatment responses we measured kinase activity in these four xenografts. In total 20 xenografts from treated mice and 20 xenografts from untreated mice were analyzed for kinase activity with PamGene tyrosine kinase micro arrays. MP34 (in vivo responder) and MP55 (in vivo non-responder) showed no clear reduction of overall kinase activity after Dasatinib treatment while a clear reduction of kinase activity was observed in MP41(in vivo responder) and MP46 (in vivo non-responder) after Dasatinib treatment (Figure 4a). Cell cultures of MP41 and MP46 xenografts showed a complete loss of Src phosphorylation upon Dasatinib treatment (Supplementary figure S1). Unfortunately no cell cultures of the xenografts of MP34 and MP55 have been established.

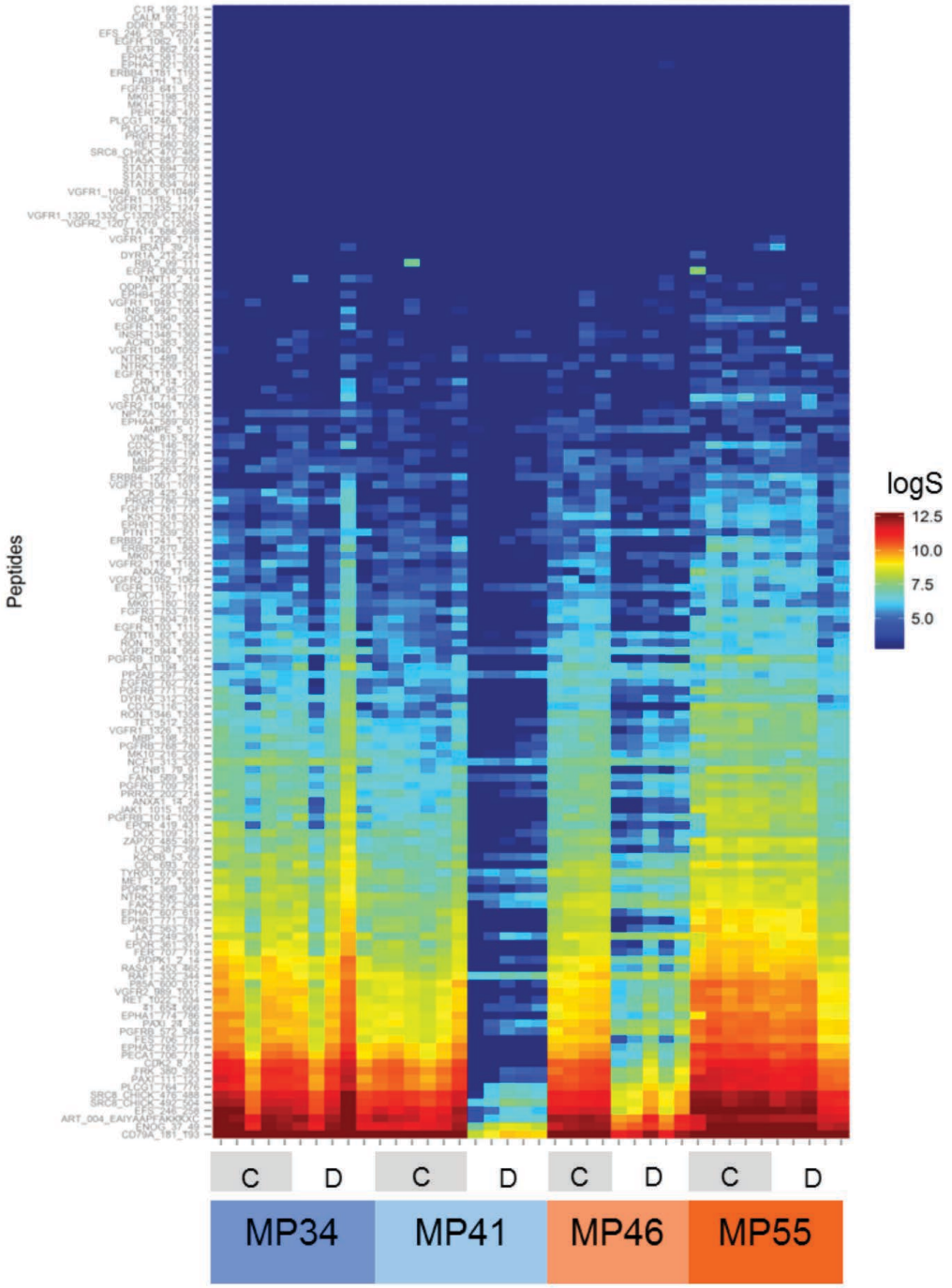
Peptides
logS
12.5
10.0
7.5
5.0
C
D
C
D
C
D
C
D
MP34
MP41
MP46
MP55

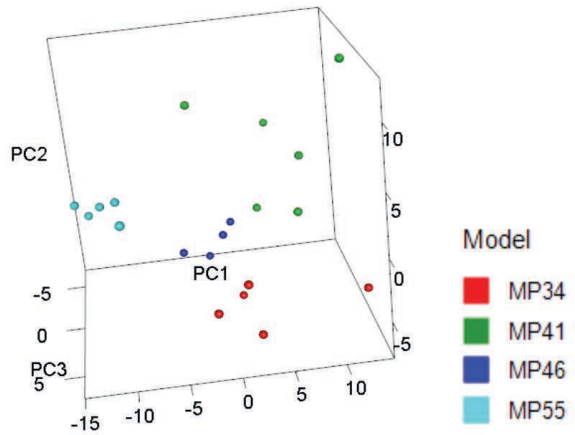

Figure 4. Kinase activity profiles after Dasatinib treatment.
(a) Heatmap visualization of PamChip kinase activity profiling results. The colors represent log-transformed kinase activity signals. Along the columns measurements on the four xenograft models are shown, for Dasatinib treated and untreated samples as indicated in the figure. The rows represent the different peptides in the analysis sorted according to their mean value over the experiment. (b) PCA analysis of the kinase activity data of the untreated xenografts. The x, y and z axis indicate the scores to principal component 1-3, respectively. Each point represents one of the 20 biological replicates in the experiment, and the coloring is according to the xenograft model they are derived from (see legend). Clustering of the replicates of the respective models is observed in the graph.

Biomarker analysis in xenografts

To investigate a possible role for kinase activity profiles as a biomarker signature for Dasatinib treatment response we assessed basal kinase activity in all four xenograft models (Supplementary figure S2). Based on basal kinase activity profiles we were able to differentiate between tumors. With PCA analysis we visualized kinase activity measurements of individual samples in a reduced 3D space. It may be seen that biological replicates derived from the same model cluster together (Figure 4b). Furthermore we compared basal kinase activity profiles with treatment efficacy. Since MP55 (highest kinase activity) was Dasatinib resistant and MP41 (lowest kinase activity) was most prone to Dasatinib treatment, we suggest a possible correlation between basal kinase activity and treatment efficacy.

DISCUSSION

Src has previously been identified as an important kinase involved in UM growth via activation of the MAPK pathway [12]. Moreover, Src may be an intermediate in oncogenic signaling by mutant *GNAQ* and *GNA11* that are almost uniquely correlated with UM

development. Based on this, we performed preclinical analysis with Dasatinib, a Src family-kinase inhibitor that is already used clinically in treating leukemia [14].

Using seven early passage primary UM cell cultures, we analyzed whether UM cell growth could be inhibited using Dasatinib. In four out of seven UM cultures, cell proliferation was reduced after treatment with Dasatinib whereas the remaining cultures appeared unaffected. Results were obtained up to three days after treatment so possibly different results would be found when incubation time was prolonged. To investigate the underlying mechanism, MAPK activation in response to Dasatinib treatment was analyzed. Remarkably, growth responders as well as non-responders displayed decreased pERK after treatment with Dasatinib. To find an explanation, potential molecular biomarkers in UM were evaluated. Both *GNAQ* and *GNA11* mutations as well as a wildtype genotype were detected in the responders. Monosomy 3, on the other hand, appeared to correlate loosely with growth inhibition as two out of four responders displayed loss of chromosome 3, while none of the non-responders showed monosomy 3.

Similar to the in vitro cell cultures, UM xenografts responded variably to Dasatinib treatment. Four tumor xenografts were evaluated of which 2 were considered responders since both tumor growth and kinase activity significantly decreased upon treatment. Based on tumor growth also 2 non-responders were identified. Additionally, we analyzed each mouse individually, showing treatment effects in 84% of the xenografts. Next, basal kinase activity was evaluated as biomarker for Dasatinib treatment. Based on their kinase activity all biological replicates of each xenograft clustered together in statistical analysis. Remarkably, the tumor (MP55) with the highest basal kinase activity appeared to be the most resistant to Dasatinib treatment. Even though sample size is limited, we suggest that tumor kinase activity should be investigated as a potential biomarker for Dasatinib treatment. Recently, phase I/II trials with Dasatinib were performed on melanomas including ocular melanomas [19]. Since Dasatinib is poorly tolerated at high doses, the need for biomarker research and optimized treatment is a necessity [20]. In the future, prophylactic adjuvant treatment of high-risk patients could be a possibility, hence biomarker analysis should be performed on both patients treated locally and patients treated with enucleation. Assessment of chromosome 3 status by fine-needle-aspiration biopsy has been found to be feasible in patients undergoing brachytherapy [21]. However, analyses of biopsies will only become clinically relevant if promising treatment options for metastases patients would become available.

In summary, we have shown that in a number of UM, Dasatinib inhibits cell growth in vitro and in vivo. However, growth response could not be correlated with molecular markers

such as *GNAQ/GNA11* mutations and monosomy 3. Though, our data indicate that general kinase activity can be a biomarker for responsiveness to Dasatinib treatment.

[1] Singh AD, Bergman L, Seregard S. Uveal melanoma: Epidemiologic aspects. Ophthalmol Clin North Am. 2005;18(1):75–84. https://doi.org/10.1016/j.ohc.2004.07.002.

[2] Damato B. Detection of uveal melanoma by optometrists in the United Kingdom. Ophthalmic Physiol Opt. 2001;21(4):268–71. https://doi.org/10.1046/j.1475-1313.2001.00595.x.

[3] Kujala E, Mäkitie T, Kivelä T. Very Long-Term Prognosis of Patients with Malignant Uveal Melanoma. Investig Ophthalmol Vis Sci. 2003;44(11):4651–9. https://doi.org/10.1167/iovs.03-0538.

[4] Augsburger JJ, Corrêa ZM, Shaikh AH. Effectiveness of Treatments for Metastatic Uveal Melanoma. Am J Ophthalmol. 2009;148(1):119–27. https://doi.org/10.1016/j.ajo.2009.01.023.

[5] Van Raamsdonk CD, Bezrookove V, Green G, Bauer J, Gaugler L, O'Brien JM, et al. Frequent somatic mutations of GNAQ in uveal melanoma and blue naevi. Nature. 2009;457(7229):599–602. https://doi.org/10.1038/nature07586.

[6] Van Raamsdonk CD, Griewank KG, Crosby MB, Garrido MC, Vemula S, Wiesner T, et al. Mutations in GNA11 in uveal melanoma. N Engl J Med. 2010;363(23):2191–9. https://doi.org/10.1056/NEJMoa1000584.

[7] Wu X, Li J, Zhu M, Fletcher JA, Hodi FS. Protein kinase C inhibitor AEB071 targets ocular melanoma harboring GNAQ mutations via effects on the PKC/Erk1/2 and PKC/NF-κB pathways. Mol Cancer Ther. 2012;11(9):1905–14. https://doi.org/10.1158/1535-7163.MCT-12-0121.

[8] Chen X, Wu Q, Tan L, Porter D, Jager MJ, Emery C, et al. Combined PKC and MEK inhibition in uveal melanoma with GNAQ and GNA11 mutations. Oncogene. 2014;33(39):4724–34. https://doi.org/10.1038/onc.2013.418.

[9] Babchia N, Calipel A, Mouriaux F, Faussat AM, Mascarelli F. The PI3K/Akt and mTOR/P70S6K signaling pathways in human uveal melanoma cells: Interaction with B-Raf/ERK. Investig Ophthalmol Vis Sci. 2010;51(1):421–9. https://doi.org/10.1167/iovs.09-3974.

[10] Triozzi PL, Eng C, Singh AD. Targeted therapy for uveal melanoma. Cancer Treat Rev. 2008;34(3):247–58. https://doi.org/10.1016/j.ctrv.2007.12.002.

[11] Zuidervaart W, Van Nieuwpoort F, Stark M, Dijkman R, Packer L, Borgstein AM, et al. Activation of the MAPK pathway is a common event in uveal melanomas although it rarely occurs through mutation of BRAF or RAS. Br J Cancer. 2005;92(11):2032–8. https://doi.org/10.1038/sj.bjc.6602598.

[12] Maat W, Filali M El, Dirks-Mulder A, Luyten GPM, Gruis NA, Desjardins L, et al. Episodic Src activation in uveal melanoma revealed by kinase activity profiling. Br J Cancer. 2009;101(2):312–9. https://doi.org/10.1038/sj.bjc.6605172.

[13] Shi H, Zhang CJ, Chen GYJ, Yao SQ. Cell-based proteome profiling of potential Dasatinib targets by use of affinity-based probes. J Am Chem Soc. 2012;134(6):3001–14. https://doi.org/10.1021/ja208518u.

[14] Shah NP, Tran C, Lee FY, Chen P, Norris D, Sawyers CL. Overriding imatinib resistance with a novel ABL kinase inhibitor. Science (80-). 2004;305(5682):399–401. https://doi.org/10.1126/science.1099480.

[15] Talpaz M, Shah NP, Kantarjian H, Donato N, Nicoll J, Paquette R, et al. Dasatinib in Imatinib-Resistant Philadelphia Chromosome–Positive Leukemias. N Engl J Med. 2006;354(24):2531–41. https://doi.org/10.1056/nejmoa055229.

[16] Hantschel O, Rix U, Superti-Furga G. Target spectrum of the BCR-ABL inhibitors imatinib, nilotinib and dasatinib. Leuk. Lymphoma, vol. 49, Leuk Lymphoma; 2008, p. 615–9. https://doi.org/10.1080/10428190801896103.

[17] Lindauer M, Hochhaus A. Dasatinib. Recent Results Cancer Res. 2010;184:83–102. https://doi.org/10.1007/978-3-642-01222-8_7.

[18] Némati F, Sastre-Garau X, Laurent C, Couturier J, Mariani P, Desjardins L, et al. Establishment and characterization of a panel of human uveal melanoma xenografts derived from primary and/or metastatic tumors. Clin Cancer Res. 2010;16(8):2352–62. https://doi.org/10.1158/1078-0432.CCR-09-3066.

[19] Algazi AP, Weber JS, Andrews SC, Urbas P, Munster PN, Deconti RC, et al. Phase i clinical trial of the Src inhibitor dasatinib with dacarbazine in metastatic melanoma. Br J Cancer. 2012;106(1):85–91. https://doi.org/10.1038/bjc.2011.514.

[20] Kluger HM, Dudek AZ, McCann C, Ritacco J, Southard N, Jilaveanu LB, et al. A phase 2 trial of dasatinib in advanced melanoma. Cancer. 2011;117(10):2202–8. https://doi.org/10.1002/cncr.25766.

[21] Shields CL, Ganguly A, Materin MA, Teixeira L, Mashayekhi A, Swanson LA, et al. Chromosome 3 analysis of uveal melanoma using fine-needle aspiration biopsy at the time of plaque radiotherapy in 140 consecutive cases. Trans Am Ophthalmol Soc. 2007;105:43–52.

SUPPLEMENTARY FIGURES

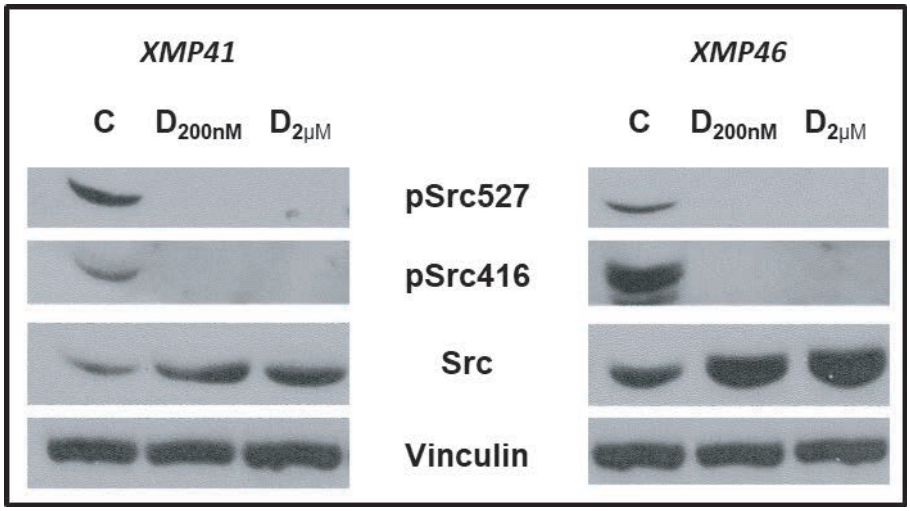

Figure S1.

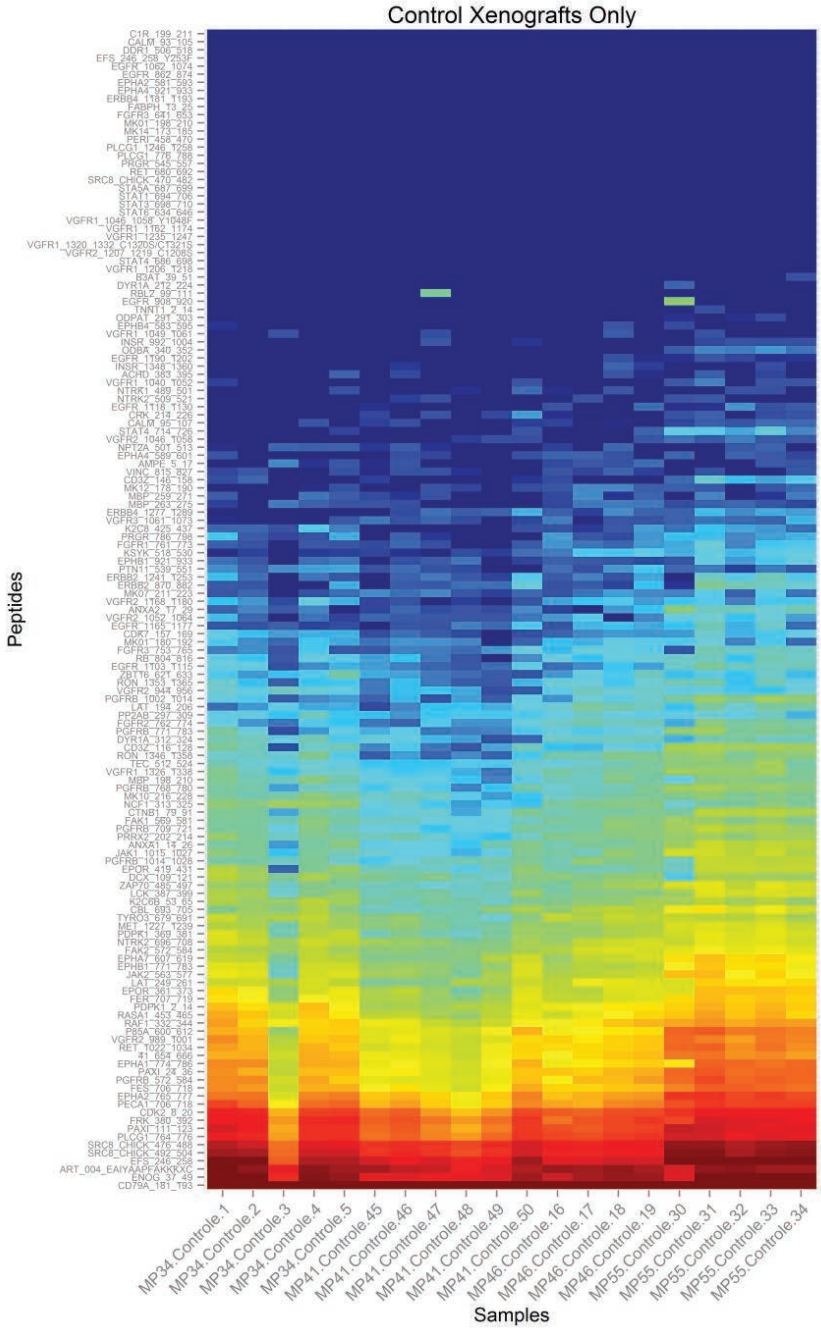
Control Xenografts Only
Peptides
Samples
mpval
12.5
10.0
7.5
5.0
MP34.Controle.1
MP34.Controle.2
MP34.Controle.3
MP34.Controle.4
MP34.Controle.5
MP41.Controle.45
MP41.Controle.46
MP41.Controle.47
MP41.Controle.48
MP41.Controle.49
MP41.Controle.50
MP46.Controle.16
MP46.Controle.17
MP46.Controle.18
MP46.Controle.19
MP55.Controle.30
MP55.Controle.31
MP55.Controle.32
MP55.Controle.33
MP55.Controle.34

Figure S2.